# Optimal Energy Efficiency Evaluation in Induction Machines Driven by Adjustable Speed Drives under EN 50598-2 and IEC 61800-9-1 Standards

Kevin Lee Peter Zhai Thomas Ruchti Benjamin Haberkorn Joseph Zhou

Electrical Sector
Eaton Corporation
Menomonee Falls, Wisconsin, USA

***Abstract*—The European Commission has defined a sustainable energy industry as a core 2030 strategy: cut $CO_2$ emissions by 40% throughout Europe. Energy-saving adjustable speed drive (ASD) solutions play a key role in this effort. As the regulatory requirements continue to grow, it is imperative to have common quantifiable standards. Therefore, a systematic approach is proposed in the European EN 50598-2 and International IEC 61800-9-1 standards in order to determine and verify the efficiency of the complete drive module (CDM) and the power drive system (PDS). As compared with the benchmarked linear Volts/Hz profile, three types of energy saving algorithms representing industry practices including scalar quadratic Volts/Hz control, flux optimization, and scalar energy optimizing Volts/Hz algorithm are presented for quantifying their performances. In variable torque (VT) applications, due to its low computational burden, stable operation, insensitivity and demonstrated energy saving effectiveness, the efficiency optimizing Volts/Hz control method is selected for developing evaluation procedures under EN 50598-2 and IEC 61800-9-1 Standards. Experimental tests with a 400V, 50Hz, 7.6A ASD and a 4.6kW, 380V, 50Hz IM system are conducted for quantifying the losses and energy efficiency applying the efficiency optimizing Volts/Hz strategy. The methodology and evaluation procedures presented in this paper provide reference value and clarity for practicing engineers.**

***Keywords—induction machine, adjustable speed drive, optimal energy efficiency control algorithms, energy efficiency standards.***

## I. INTRODUCTION

Although numerous research findings have been published relative to achieving additional energy savings for adjustable speed driven (ASD) induction machine (IM) loads, only recently the global industry has published governing energy efficiency standards such as EN 50598-2[1] and IEC 61800-9-1[2]. For voltages < 1kV and power ratings up to 1MW, they define the procedures and operating points for determining ASD system losses and energy efficiency classes. The predefined converters and systems are used to compare losses for categorizing energy efficiency classes. These standards have been gradually adopted by ASD and IM manufacturers in the European Committee of Manufacturers of Electrical Machines and Power Electronics (CEMEP) and the National Electrical Manufacturers Association (NEMA) in North America. Algorithms have been developed to operate under either field oriented control (FOC), direct torque control (DTC), or scalar Volts/Hz control mode. In each IM control mode, different strategies are proposed. A pioneering work patented in [3] proposed a method for maximizing power factor, in order to reduce IM input power. It was derived in [4] that the optimal IM slip for energy efficiency is higher than the slip at the minimum motor current, and is typically very close to the rated motor slip. Using motor current as a control variable rather than the input power, a scalar control was described in [5]. In [6], a power factor control, a model-based control, and a search control were implemented experimentally for both FOC and scalar motor drives. The effect of flux optimization with DTC was discussed in [7]. Expected savings using Volts/Hz loss minimization was studied in [8]. The energy efficiency outcomes from these publications vary significantly, partly due to a lack of industry standards to quantify their effectiveness in the past. The newly introduced EN 50598-2 and IEC 61800-9-1 standards make it possible now to evaluate complete drive module (CDM) and power drive system (PDS) losses and efficiency of an ASD driven IM load system, helping clarify which algorithm could be most advantageous in real world applications.

The new contributions and objectives of this paper are three folds:

(a). Categorize and analyze industry dominating energy efficiency algorithms in three groups: (1). Scalar quadratic Volts/Hz control; (2). Flux optimization in FOC; (3). Scalar energy optimizing Volts/Hz control. Comparable experimental evaluations on energy efficiency performances are presented;

(b). Demonstrate that an energy optimizing Volts/Hz control can achieve good energy efficiency in practical applications;

(c). Present the comparable CDM and PDS energy efficiency results and data analytics under the frame work of EN 50598-2 and IEC 61800-9-1 Standards.

System descriptions with intrinsic energy saving potentials in variable torque (VT) mode are highlighted in Section II. In pump, fan and compressor applications, up to 70 percent of electricity costs can be saved through the use of efficient ASD technology. Using a baseline for energy efficiency comparison as a benchmark, theoretical models of three categorized algorithms and the governing standards are described in Section III. The quadratic Volts/Hz profile is easier to implement and can provide reduction on overall losses until the system becomes unstable in a higher load demanding scenario.

978-1-4799-7312-5/18/$31.00 ©2018 IEEE

A digital simulation case study of a 7.5kW, 480V, 60Hz ASD and IM system is demonstrated to illustrate the quadratic Volts/Hz method's limitation. The experimental implementation at an input power level of 400V, 50Hz, 7.6A, evaluation procedures, test results and data analytics are presented in Section IV for energy optimizing Volts/Hz control. The summary of contributions and conclusions is presented in Section V.

## II. System Descriptions for Achieving Energy Efficiency Optimization

The block diagram in Fig. 1.(a) shows the overall system architecture. The IM and fan/pump load are driven by an ASD, which controls the IM torque and speed. In the system energy efficiency optimization implementation, the ASD records IM currents and voltages, power consumption and speed. The ASD controller module takes these values as inputs, executes the energy efficiency optimization algorithm, which can be based on FOC or Volts/Hz control mode. The algorithm generates the PWM outputs from the ASD power structure to control the IM accordingly. Fig. 1.(b) is the per phase IM equivalent circuit in steady state operation, where:

$R_s$, $R_r$ are stator and rotor resistances, $s$ is IM slip ;

$L_{ls}$, $L_{lr}$ are stator and rotor leakage inductances;

$L_m$, $R_m$ represent magnetizing inductance and resistance;

$V_s$, $i_s$, $i_r$ are stator voltage, stator and rotor currents.

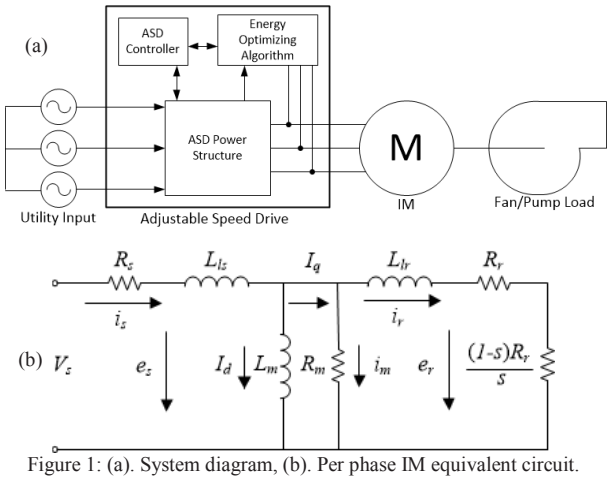


Figure 1: (a). System diagram, (b). Per phase IM equivalent circuit.

Fig. 2 illustrates affinity laws governing VT fan and pump applications. For a given fan or pump geometry, Eq. (1) defines how flow, static pressure (SP), and power vary with two IM shaft speeds from $\omega_1$ to $\omega_2$.

$$\frac{Flow_1}{Flow_2} = \frac{\omega_1}{\omega_2}, \quad \frac{SP_1}{SP_2} = \left(\frac{\omega_1}{\omega_2}\right)^2, \quad \frac{Power_1}{Power_2} = \left(\frac{\omega_1}{\omega_2}\right)^3 \qquad (1)$$

When the IM speed is reduced to 50% of the full speed, the mechanical power can decrease to approximately 12.5% of its original value, demonstrating the dramatic and inherent energy savings benefit of using an ASD, especially in VT applications.

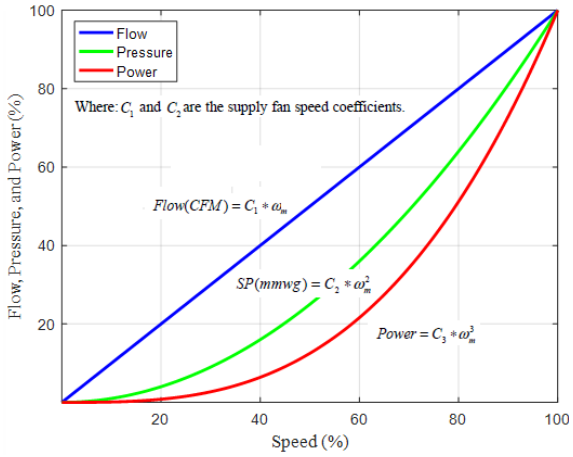


Figure 2: Affinity laws for pumps and fans in variable torque (VT) mode.

However, in an actual system, overall system efficiency drops significantly at reduced shaft speed and/or partial load torque due to a disproportionate increase in losses. The energy efficiency optimization algorithms implemented in this paper can help achieve additional energy savings in such a scenario.

## III. Energy Efficiency Optimization Algorithms and Industry Standards

### *A. Baseline Benchmark for Comparative Evaluation of Energy Efficiency Algorithms*

In applications such as heating, ventilating and air conditioning (HVAC), scalar Volts/Hz control mode dominates the industry, due to its simplicity and economic benefits. But, a linear Volts/Hz curve typically provides a voltage higher than necessary, resulting in wasted energy, especially when the reference frequency is significantly lower than the rated frequency. IM core losses are mainly composed of losses caused by eddy current and hysteresis in the iron core, and are typically proportional to the square of the input voltage. Applying unnecessarily high voltage to the motor generates excessive motor core losses in the form of heat and noise. To quantify the effectiveness of energy efficiency optimization, the linear Volts/Hz is defined as a baseline, providing a benchmark for evaluating three different algorithms: (a). Scalar quadratic Volts/Hz curve; (b). Flux optimization based on FOC; (c). Scalar energy optimizing Volts/Hz control.

### *B. Scalar Quadratic Volts/Hz Algorithm*

Most ASDs are equipped with this feature. The voltage output at any given frequency is lower than the voltage output based on the linear Volts/Hz curve, which tends to achieve a higher level of energy saving as long as the load demand is under control. When the IM load is higher than what the static voltage can sustain in a stable manner, this control method could result in system instability, higher IM output currents with overheating or stalling the IM altogether.

A case study is illustrated in Figs. 3 and 4, with an ASD driving a 7.5kW, 460V, 60Hz IM with a rated current of 12.9A, rated torque of 41.4NM, and rated speed of 1728RPM.

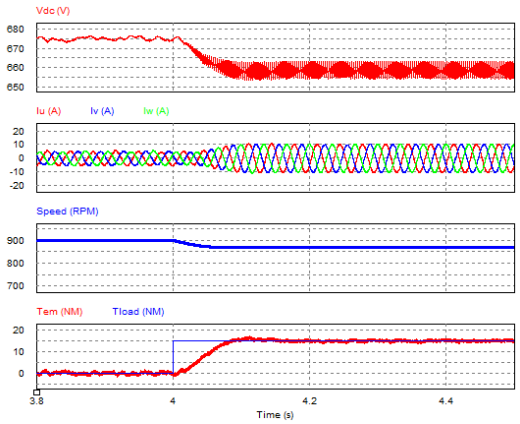


Figure 3: Performance with linear Volts/Hz curve. From top to bottom: dc link voltage, IM currents, speed, commanded and actual torques.

In Fig. 3, the operating conditions are 480V ASD input in linear Volts/Hz mode, at half speed with a step load change from no load to a partial load of 15NM at 4s. The dc link voltage, IM currents, speed, and load torque all settle in their respective and expected steady state equilibriums. There is enough IM output voltage maintaining the required load level.

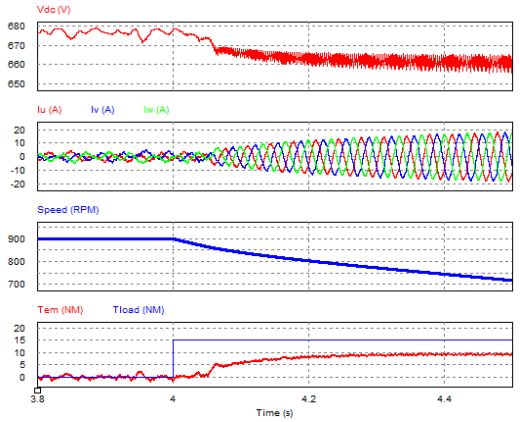


Figure 4: Performance with quadratic Volts/Hz curve. From top to bottom: dc link voltage, IM currents, speed, commanded and actual torques.

The quadratic Volts/Hz operation is activated at 4s in Fig. 4, where the load requirement cannot be sustained. This is the situation in which the energy efficiency improvement cannot be achieved. The quadratic Volts/Hz algorithm is only effective in reduced load instances, limiting its usefulness in a dynamic operating environment.

### *C. Flux Optimization Algorithm based on FOC*

In FOC, the IM equivalent circuit of Fig. 1.(b) can be interpreted in dq synchronous reference frame representation as in Fig. 5. The IM losses ($P_{loss}$) are defined in Eq. (2), consisting of three components.

$$P_{loss} = P_s + P_r + P_c = R_s \cdot \left(I_d^2 + I_q^2\right) + R_r \cdot \left(I_q - \frac{\omega_s \cdot L_m}{R_m} \cdot I_d\right)^2 + \frac{(\omega_s \cdot L_m)^2}{R_m} \cdot I_d^2 \quad (2)$$

Where: $P_s$ , $P_r$, and $P_c$ are stator, rotor and core losses respectively. $\omega_s$ is synchronous angular velocity.

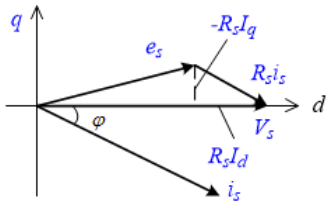


Figure 5: Vector diagram of Figure 1 (b).

The strategy for higher energy efficiency is to determine the voltage and frequency to be applied to the IM with minimum losses. There is a unique combination of $I_d$ and $I_q$ current components that provides the minimum IM losses for each operating condition.

Regrouping Eq. (2) and defining the losses in dq synchronous reference frame as:

$$P_d = \left[\frac{\omega_s^2 L_m^2}{R_c}\left(1 + \frac{R_r}{R_c}\right) + R_s\right] I_d^2 \quad (3)$$

$$P_q = (R_s + R_r) I_q^2 \quad (4)$$

Accordingly, each loss component is expressed in terms of the stator current components, and the optimum condition is obtained from the differentiation of the total loss with respect to the coefficient $A$ as defined in Eq. (3). The optimum value of $A$ is labeled as $A_{opt}$ that determines the appropriate flux level which is often less than the rated value in lower IM speed and lighter load operating conditions. As such, the overall IM system energy efficiency is kept as high as possible.

It can be derived [6, 10] that when $P_d = P_q$, the minimum losses in flux optimization can be obtained as in Eq. (5).

$$A = \frac{I_q}{I_d}, \quad \frac{\partial P_{loss}}{\partial A} = 0, \quad A_{opt} = \sqrt{\frac{\frac{(\omega_s \cdot L_m)^2}{R_m}\left(1 + \frac{R_r}{R_m}\right) + R_s}{R_r + R_s}} \quad (5)$$

The flux optimization implementation is illustrated in the block diagram of Fig. 6. The IM losses are minimal when the loss in rotor flux direction is equal to its quadrature quantity.

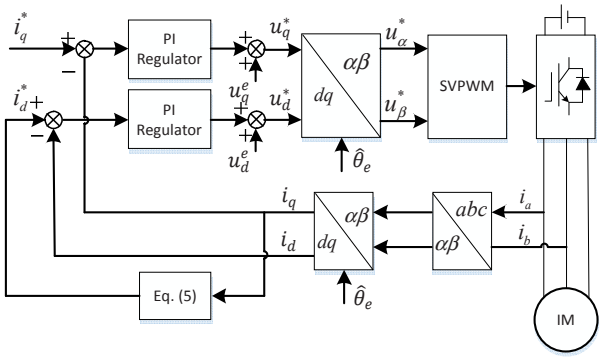


Figure 6: FOC system block diagram in flux optimization implementation.

Since the IM parameters are required in this FOC method, the results can be sensitive to parameter variation over operating conditions and time. The computation burden is the highest among all methods described in this paper.

*D. Scalar Energy Optimizing Volts/Hz Control Algorithm*

In linear Volts/Hz mode, the maximum IM efficiency is typically at full load with rated slip. In VT applications such as HVAC or pumps, light load operation at lower speed is common. Two phenomena occur:

(1). The slip decreases further from its rated value as the load reduces;

(2). Even though the full IM torque is not required, the full magnetizing current still exists. It produces excessive magnetic field and reactive current that contribute to IM core and winding losses, generating heat and wasting energy.

In order to overcome the shortcomings of the linear Volts/Hz profile, an optimal approach can be implemented. Figs. 7 and 8 illustrate the energy optimizing Volts/Hz control concept. In Fig. 7, by keeping the same load torque $T_r$ and speed $\omega_r$, while the IM voltage is reduced, the slip increases accordingly.

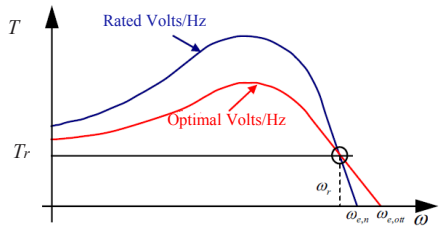


Figure 7: Optimal Volts/Hz control Scenario.

In the case of quadratic Volts/Hz, it could accomplish a similar goal in terms of improving IM efficiency, except that there is a stability and optimization limitation as described in Section III.(B). Fig.8 demonstrates two degrees of freedom (DOF) in the energy optimizing Volts/Hz control:

(a). Change IM output voltage (moving up and down);

(b). Change slip (moving left and right).

Very often, the slip can be increased to be near its rated value, and the voltage is adjusted to reduce the magnetic field and magnetizing current. The overall system can still meet the load requirements, and optimal energy efficiency is achieved while maintaining the IM system stability.

The theoretical explanation for the energy saving capability in Figs. 7 and 8 is analyzed. The IM shaft output power is expressed in Eq. (6), while the IM torque and slip are defined in Eq. (7). In this energy optimizing Volts/Hz control mode, the magnetizing current is minimized. Thus, neglecting $I_d$ and $i_m$ due to a large $R_m$ in Fig. 1(b), the rotor current is derived from complex vectors as in Eq. (8). The output power is calculated in Eq. (9). Furthermore, neglecting insignificant terms in Eqs. (8) and (9), the load current is proportional to the stator voltage $V_s$. Concurrently, $P_{out}$ is proportional to $V_s$ squared, which impacts the power consumption most notably.

$$P_{out} = 3 \times \frac{i_r^2 \cdot R_2 \cdot (1-s)}{s} = T_e \cdot \omega_{rm} \tag{6}$$

Where $\omega_{rm}$ is mechanical speed (rad/s), $\omega_r$ is electrical speed (rad/s), $s$ is IM slip.

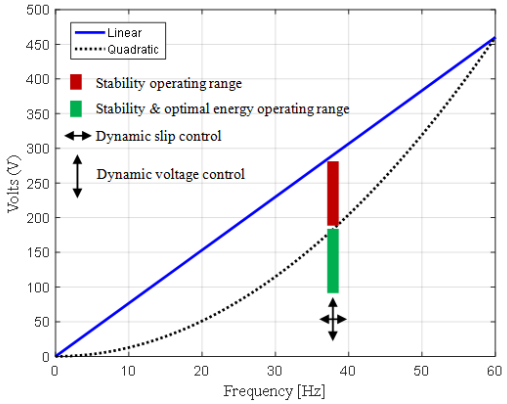


Figure 8: Energy optimizing Volts/Hz control strategy.

$$T_e = \frac{P_{out}}{\omega_{rm}} = \frac{3p}{2} \times \frac{i_r^2 \cdot R_2 \cdot (1-s)}{s \cdot \omega_r} \tag{7}$$

Where $s = \frac{\omega_e - \omega_r}{\omega_e}$, and $\omega_r = \omega_e \cdot (1-s)$.

$$i_r \approx \frac{V_s^2}{\sqrt{\left(R_s + \frac{R_r}{s}\right)^2 + \left(\omega_r \cdot L_s + \omega_r \cdot L_r\right)^2}} = \tag{8}$$

$$V_s \times \frac{1}{\sqrt{\left(R_s + \frac{R_r}{s}\right)^2 + \left(\omega_r \cdot L_s + \omega_r \cdot L_r\right)^2}} \propto \frac{V_s}{\omega_e}$$

$$P_{out} = 3 \times \frac{V_s^2}{\left(R_s + \frac{R_r}{s}\right)^2 + \left(\omega_r \cdot L_s + \omega_r \cdot L_r\right)^2} \times \frac{R_2 \cdot (1-s)}{s} \propto \left(\frac{V_s}{\omega_e}\right)^2 \tag{9}$$

The flowchart of the energy optimizing Volts/Hz is shown in Fig. 9. The system can start with a linear Volts/Hz profile, then during operation, IM data such as voltages, currents, speed and power can be acquired. With the objective to maximize the system energy efficiency, while meeting load requirements and maintaining stability, the energy optimizing Volts/Hz algorithm based on Figs. 7 and 8 is activated.

Other advantages of the scalar energy optimizing Volts/Hz control platform include:

(1). Plug and play with ease of use: It does not require user intervention due to the use of automatic adjustment;

(2). It is insensitive to IM parameter variation, as compared to the FOC based flux optimization method in Section III.(C);

(3). It is computationally efficient.

*E. European EN 50598-2 Standard and International IEC 61800-9-1 Standard for Energy Efficiency*

EN 50598-2 [1] was proposed by CEMEP. It defines energy efficiency indicators for CDM such as an ASD and PDS which is formed by CDM and motor load. The standard includes a methodology to determine the CDM and PDS losses, assigning the IE and IES values, which apply to motor driven equipment from 0.12 to 1,000 kW (100 to 1,000 V).

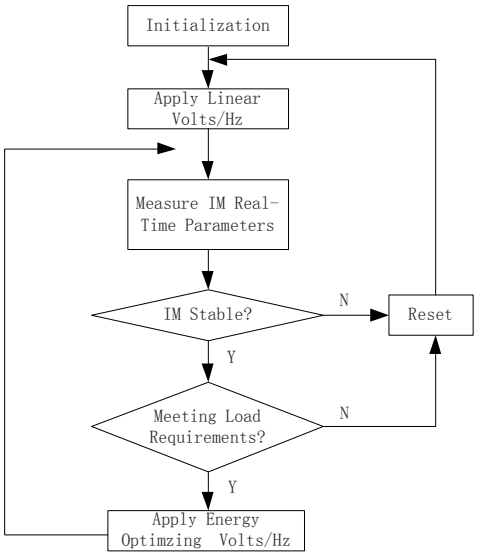


Figure 9: Flowchart of linear and energy optimizing Volts/Hz modes.

Efficiency can be determined by testing or in conjunction with elaborate models for calculating inverter and reference motor losses. International Electro-technical Commission (IEC) adopted this standard and published 61800-9-1 [2] as an international standard in 2017. The evaluation of energy efficiency algorithm optimization is quantified according to Fig. 10.

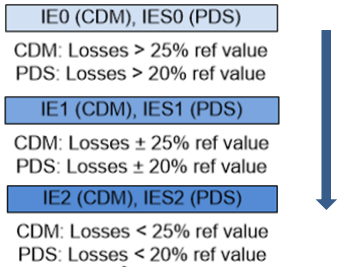


Figure 10: IE and IES energy efficiency classification for CDM and PDS.

*E.(A). IE Class in CDM*

The CDM efficiency class (IE) is determined by the ratio of the CDM losses to its reference losses [1]. The operating points for determining relative power losses are depicted in Fig. 11.

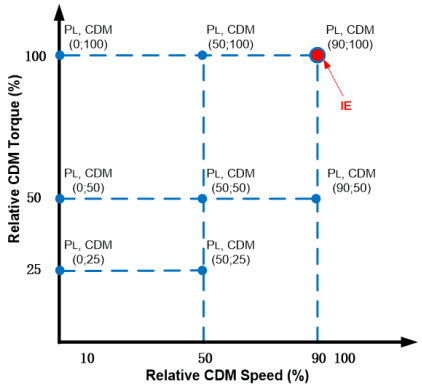


Figure 11: Relative CDM power loss operating points.

- Depending on the CDM power rating, the load current and displacement power factor are specified as a hypothetical test motor;
- There are eight operating points with a maximum frequency of 90% of rated value. It is chosen such that the CDM over-modulation region can be avoided;
- The CDM IE class is determined by the relative losses at the point of 90% speed and 100% torque;
- The relative losses at the other seven points are specified in the product documentation, which are independent of the IE class definition.

*E.(B). IES Class in PDS*

The PDS efficiency class (IES) is determined by the ratio of the PDS losses to its reference losses [1]. The operating points for determining relative power losses are shown in Fig. 12.

- There are also eight operating points with a maximum frequency of 100% of its rated value;
- The PDS IE class is determined by its relative losses at the point of 100% speed and 100% torque;
- IES2 is the best efficiency class as defined in Fig. 10, which is achieved if a PDS has <20% of the reference PDS losses;
- While the CDM IE rating is stated on the nameplate, the PDS IES rating is provided in product installation and maintenance manuals.

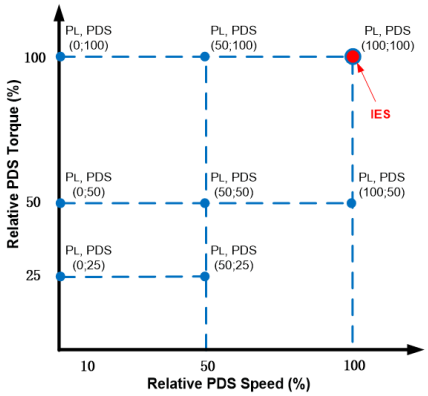


Figure 12: Relative PDS power loss operating points.

*E.(C). Reference Motor Definition*

A reference motor is defined by mathematical equations and/or power losses, used as a basis for comparing with other motors. As such, it might not be an available product on the market, it might be a generally available product from all concerned manufacturers. It may be as simple as any motor which has the required voltage and power ratings, or the next preferred rating above that of the converter. An electronic load is a possibility to simplify testing.

- In order to determine losses or efficiency classes of a complete system, the CDM user needs data from the motor manufacturer or reference values as given in 5.3.3 in [1];
- Efficiency classes for sinusoidal fed asynchronous induction machines are defined in EN 60034-30-1.

The classification is conducted for rated output ($P_n$: 100 % torque, $n_n$:100 % speed);

- The losses for the reference motor are derived from 4 pole asynchronous motors, using the 50Hz (applies to 60Hz as well), IE2 efficiency values according to EN 60034-30-1;
- The inverter introduces a multiplier of $r_{HL}$ due to additional harmonic losses: $r_{HL}$=0.15 for motors with a rated output power up to 90kW, $r_{HL}$=0.25 for motors with a rated output above 90kW.

## IV. Experimental Results and Analysis

### *A. Experimental Evaluation on Energy Saving Algorithms*

For the 20HP, 480V, 60Hz system, the ASD delivers power to the IM, which in turn drives a size 24½ blower fan [11]. Taking the linear Volts/Hz control as a benchmark, three energy saving algorithms: quadratic, flux optimization and energy optimizing V/Hz control, as described in Section III, are implemented for a half load testing. At each operating mode, five adjustable frequency points are selected in the range between 30Hz and 55Hz. At each combination of frequency and operating mode, power consumption, temperature, IM speed, static pressure and atmospheric pressure are captured. Using linear Volts/Hz mode as a benchmark, it is demonstrated in Fig. 13 that the scalar Volts/Hz based energy efficiency optimization has larger energy savings than the other two methods.

Based on the test results, the energy optimizing Volts/Hz control mode is selected as the candidate for further evaluation under EN 50598-2 and IEC 61800-9-1 standards.

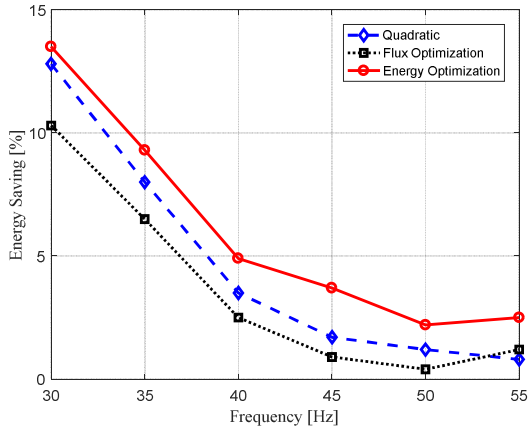


Figure 13: Experimental results of various energy saving algorithms as compared with a benchmark linear Volts/Hz baseline.

### *B. Experimental Setup in Accordance with EN 50598-2 Standard and IEC 61800-9-1 Standard*

The ASD input and output powers are measured to evaluate the CDM efficiency and its IE class, while the ASD input power and mechanical shaft power output are recorded to quantify the PDS energy efficiency and its IES class. Fig. 14 illustrates the overall measurement system architecture, with the boundary definitions of ASD as a CDM, as well as a combined ASD and IM to form a PDS.

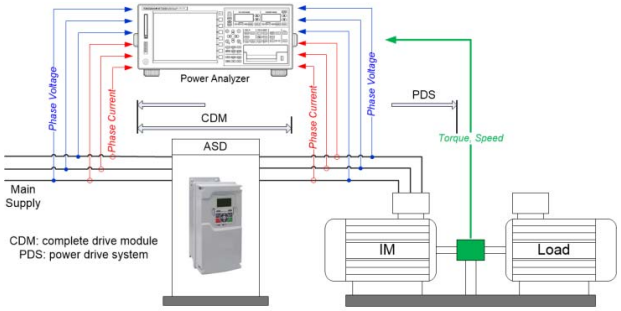


Figure 14: Experimental setups with measurement points in CDM and PDS definitions.

Due to the harmonic content of the pulse width modulation (PWM) output waveform produced by ASDs, it can be challenging to obtain accurate and reliable system losses and efficiency measurement. Leveraging capability of ASDs to carry out loss segregation tests is investigated in [9]. Although it has potential to make measurements when elaborate test equipment is not available, further agency validation and certification are required for its acceptance. In this paper, certified test equipment and procedures are used in all data acquisition. Fig. 15 shows the test equipment including the precision power analyzer of WT3000 from Yokogawa [12].

Figure 15: Experimental setup of 4.6kW ASD system with data acquisition using Yokogawa WT3000 precision power analyzer.

Table I is a subset of test load displacement factor between fundamental output current and fundamental output voltage at different points of operation in [1]. A reference IE2 IM of 4.6kW, 460V, 60Hz is chosen in order to meet the test requirement for compliance with the standards [1-2].

Table I. Test Load Displacement Factor between Fundamental Output Current and Fundamental Output Voltage [1].

| Torque producing current (/%) | Test load displacement factor cos(ϕ) for the apparent power range of 1,29kVA (0,75kW) to <7,94kVA (5,5kW) |
|---|---|
| 25 | 0.38 |
| 50 | 0.60 |
| 75 | 0.72 |
| 100 | 0.79 |

### *C. Experimental Results and Evaluation on IE Class of CDM*

The experimental setup consists of a 400V, 50Hz, 7.6A ASD, a 4.6kW, 380V, 50Hz IM and a load control system. Since the ASD rated current is 7.6A, the actual IM load sits at 3.8kW at full load. Applicable to the operating conditions in the

experimental setup, Table II specifies the reference CDM losses that are used in the IE energy efficiency classification evaluation. Where $P_{rM}$, $S_{r\text{-}equ}$, $I_{r\text{-}out}$, $P_{L\text{-}RCDM(90,100)}$ are the reference CDM output power, apparent power, current, losses at 90% speed and 100% torque, respectively.

TABLE II. REFERENCE CDM LOSSES FOR IE CLASS 1 DEFINITION [1].

| $P_{rM}$ / kW | $S_{r\text{-}equ}$ / kVA | $I_{r\text{-}out}$ / A of the 400V RCDM | $P_{L\text{-}RCDM(90,100)}$ / % of $S_{r\text{-}equ}$ | $P_{L\text{-}RCDM(90,100)}$ / W |
|---|---|---|---|---|
| 4 | 5.85 | 8.44 | 6.39 | 374 |

Applying the reference values in Table II, IE class definition in Fig. 10, and taking into account the measurement accuracy of 0.2% as uncertainty, the measured CDM losses and calculated IE class results are summarized in Table III. $P_{L\text{-}CDM(90,100)'}$ is referenced to the actual measured kVA base.

TABLE III. EXPERIMENTAL SUMMARY OF CDM IE CLASS RESULTS.

| Volts/Hz mode | $P_{L\text{-}CDM(90,100)}$ / kW | $P_{L\text{-}CDM(90,100)'}$ / $P_{L\text{-}RCDM(90,100)}$ | IE classification |
|---|---|---|---|
| Linear | 0.098 | 0.291 < 0.75 | 2 |
| Optimized | 0.093 | 0.276 < 0.75 | 2 |

Fig. 16 shows the baseline linear Volts/Hz CDM energy efficiency contour map with variations of IM speed from 10% to 100%, and load torque from 25% to 100%. The highest efficiency (>97%) is at near full load and speed, and the lowest of 74.5% is at 10% speed, 25% load.

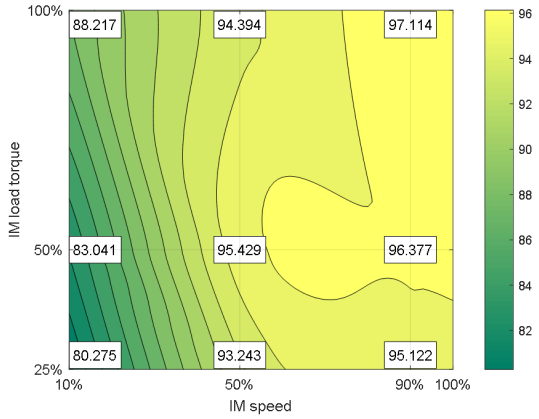


Figure 16: Experimental results of 4.6kW system: baseline CDM energy efficiency vs. IM speed and load.

### *D. Experimental Results and Evaluation on IES Class of PDS*

Both the ASD and IM losses are considered in the PDS. The reference IM meets the load power factor requirement in Table I. Additionally, Table IV defines the reference motor losses at the tested power level. The measured IM losses at the subjected operating point are 521W. Thus, the reference IM also satisfies the IE2 motor loss definition in Table IV, even after including the switching losses due to the ASD non-sinusoidal output waveforms. $P_{L\text{-}RM(100,100)}$ is the reference motor losses at 100% rated torque and speed.

TABLE IV. A SUBSET OF REFERENCE MOTOR LOSSES [1].

| $P_n$ / kW | $P_{L\text{-}RM(100,100)}$ / W |
|---|---|
| 4 | 712 |

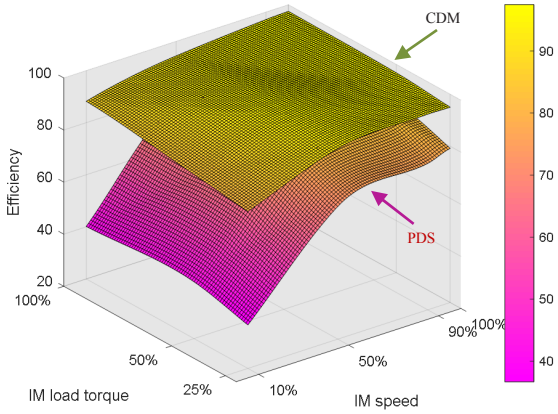


Figure 17: Experimental results of 4.6kW system: baseline CDM and PDS energy efficiency comparison vs. IM speed and load.

Fig. 17 depicts the energy efficiency surfaces comparison between the CDM and PDS. In the PDS, the highest efficiency (82.9%) is at near full load and speed, and the lowest of 31.5% is at 10% speed, 25% load. Fig. 18 illustrates the PDS energy efficiency test results with and without the energy optimizing Volts/Hz strategy enabled. The elevated surface demonstrates higher efficiency operations at light load and across a wide range of IM speed. The highest energy saving is 7.9% at 25% load and 50% speed. At near IM rated or very low speed such as 10%, as load increases, the energy saving could be less significant.

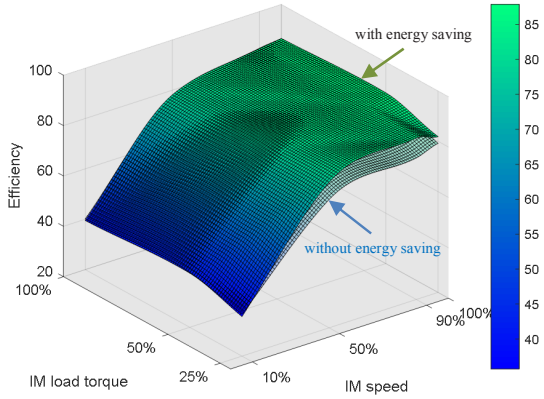


Figure 18: Experimental results of 4.6kW system: PDS energy efficiency with and without enabling energy optimizing Volts/Hz strategy.

As in the scenario for CDM, Table V specifies the reference PDS losses that are used in the IES energy efficiency classification evaluation. Where $P_{rM}$ and $P_{L\text{-}RPDS(100,100)}$ are the reference PDS output power and losses at 100% speed and 100% torque, respectively.

TABLE V. REFERENCE PDS LOSSES FOR IES CLASS 1 DEFINITION [1].

| $P_{rM}$ / kW | $P_{L\text{-}RPDS(100,100)}$ / % of $P_{rM}$ | $P_{L\text{-}RPDS(100,100)}$ / W |
|---|---|---|
| 4 | 29.11 | 1164 |

Applying the reference values in Table V, IES class definition in Fig. 10, and again taking into account the measurement accuracy of 0.2% as uncertainty, the measured PDS losses and calculated IES classification results are

summarized in Table VI. $P_{L\text{- }RPDS(100,100)'}$ is referenced to the actual measured kVA base.

TABLE VI. EXPERIMENTAL SUMMARY OF PDS IES CLASS RESULTS.

| Volts/Hz mode | $P_{L\text{- }RPDS(100,100)}$ / kW | $P_{L\text{- }RPDS(100,100)'}$ / $P_{L\text{- }RPDS(100,100)}$ | IES classification |
|---|---|---|---|
| Linear | 0.522 | 0.472 < 0.80 | 2 |
| Optimized | 0.518 | 0.468 < 0.80 | 2 |

In the above configurations, the CDM IE classification is calculated as IE2, and the PDS IES classification is determined as IES2. The CDM IE and PDS IES classification results are independent of energy saving features of the ASD.

## V. CONCLUSIONS

In this paper, the industry adopted energy saving algorithms are categorized into three groups: scalar quadratic Volts/Hz control, flux optimization in FOC or DTC, and energy optimizing Volts/Hz algorithm. The test results at half load between 30Hz to 55Hz IM speed illustrates a portion of their energy saving comparisons. Because of the ease of use and effectiveness in VT applications, the energy optimizing Volts/Hz algorithm has been selected for evaluation under EN 50598-2 and International IEC 61800-9-1 Standards. The relationship among three variables of system efficiency, IM speed, and load level is evaluated in the trend studies using 2D and 3D contour surfaces analysis. A summary of contributions and conclusions to be drawn from this paper includes the following:

- ✓ For three energy saving algorithms in modern ASDs, their theoretical models and comparative energy efficiency evaluations as functions of varying IM speed and load are presented.
- ✓ A case study on the quadratic Volts/Hz is brought up to demonstrate its energy improvement applicability and limitation in a 7.5kW ASD and IM platform.
- ✓ Although there could be other FOC based or emerging technologies for reducing PDS system losses, the energy optimizing Volts/Hz algorithm is a practiced and proven solution for achieving higher energy saving in VT applications.
- ✓ In order to obtain CDM IE and PDS IES classifications, the methodology and evaluation procedures in compliance with EN 50598-2 and International IEC 61800-9-1 Standards are described in detail.
- ✓ Based on a 400V, 50Hz, 7.6A ASD and a reference motor of 4.6kW, 380V, 50Hz IM, experimental results conclude that the CDM has a IE2 class and the PDS is IES2, regardless of whether an energy saving algorithm is activated or not.

Even though the HVAC example is highlighted in this paper, pumps, conveyors, and any application where there are extended periods of light loading can benefit from the energy optimizing Volts/Hz control algorithm. For an overall better understanding of the factors that influence energy saving outcome and standardization implication, this paper helps provide clarity in industrial control engineering and application communities.

## REFERENCES


[1] EN 50598-2: Ecodesign for power drive systems, motor starters, power electronics & their driven applications - Part 2: Energy efficiency indicators for power drive systems and motor starters, 2014.

[2] IEC 61800-9-1: Adjustable speed electrical power drive systems - Part 9-1: Ecodesign for power drive systems, motor starters, power electronics and their driven applications, 2017.

[3] F. J. Nola, "Power factor control system for ac induction motor," U.S. Patent 4,052,648, Oct. 4, 1977.

[4] T. W. Jian, N. L. Schmitz, and D. W. Novotny, "Characteristic Induction Motor Slip Values for Variable Voltage Part Load Performance Optimization," IEEE Transactions on Power Apparatus and Systems, vol. PAS-102, no. 1, pp. 38-46, 1983.

[5] I. Kioskeridis, and N. Margaris, "Loss minimization in scalar-controlled induction motor drives with search controllers," IEEE Transaction on Power Electronics, vol. 11, no. 2, pp. 213-220, 1996.

[6] F. Abrahamsen, F. Blaabjerg, J. K. Pedersen, P. Z. Grabowski, and P. Thogersen, "On the energy optimized control of standard and high-efficiency induction motors in CT and HVAC applications," IEEE Transactions on Industry Applications, vol. 34, no. 4, pp. 822–831, 1998.

[7] H. Khan, S. Hussain, and M. A. Bazaz, "Direct torque control of induction motor drive with flux optimization," International Conference on Advances in Computing, Communications and Informatics (ICACCI), pp. 618-623, 2015.

[8] A. A. C. Rebolledo, and M. A. Valenzuela, "Expected savings using loss-minimizing flux on IM drives – Part I: Optimum flux and power savings for minimum losses," IEEE Transactions on Industry Applications, vol. 51, no. 2, pp. 1408–1416, 2015.

[9] E. Agamloh, A. Cavagnino and S. Vaschetto, "Induction machine efficiency measurement using a variable frequency drive source," IEEE Energy Conversion Congress and Exposition (ECCE), pp. 768–775, 2017.

[10] G. Mirzaeva, and L. Sazdanoff, "The effect of flux optimization on energy efficiency of induction motors in fan and pump applications," Australasian Universities Power Engineering Conference (AUPEC), pp. 1-6, 2015.

[11] Industry Application IA04008001E, "Active energy control – optimum solution for maximum savings," https://www.engineeringwhitepapers.com/energy/, 2012.

[12] Yokogawa, "WT3000 precision power analyzer," https://tmi.yokogawa.com/us/library/resources/.